Nonlinear theoretical formulation of elastic stability criterion of crystal solids

Hao Wang[1,2] and Mo Li[1,*]

[1]*School of Materials Science and Engineering, Georgia Institute of Technology, Atlanta, Georgia 30332, USA*

[2]*School of Physics, Georgia Institute of Technology, Atlanta, Georgia 30332, USA*

(Received 22 November 2011; revised manuscript received 31 January 2012; published 5 March 2012)

An elastic stability criterion is generally formulated based on local elasticity, where the second-order elastic constants of a crystalline system in an arbitrary deformed state are required. While simple in formalism, such a formulation demands extensive computational effort in either an *ab initio* calculation or an atomistic simulation and often lacks clear physical interpretation. Here, we present a nonlinear theoretical formulation employing higher-order elastic constants beyond the second-order ones; the elastic constants needed in the theory are those at a zero stress state or in any arbitrary deformed state, many of which are now available. We use the published second- and higher-order elastic constants of several cubic crystals, including Au, Al, and Cu, as well as diamond-structure Si, with transcription under different coordinate frames, to test the stability conditions of these crystals under uniaxial and hydrostatic loading. The stability region, ideal strength, and potential bifurcation mode of those cubic crystals under loading are obtained using this theory. The results obtained are in good agreement with the results from the *ab initio* calculation or embedded atom method. The overall good quality of the results confirms the desired utility of this new approach to predict elastic stability and related properties of crystalline materials without involving intense computation.

DOI: 10.1103/PhysRevB.85.104103 PACS number(s): 62.20.de, 71.15.Mb, 71.55.Ak, 81.40.Jj

I. INTRODUCTION

Born formulated the elastic stability criterion in the context of thermal melting of a crystal.[1,2] It states that to ensure a crystalline solid in a stable state, the determinant of the second-order elastic constant tensor C must be positive, $|C| > 0$, which amounts to saying that given a perturbative strain η, such as in thermal melting, the variation of the internal energy of the system must remain positive and convex if the system is in a stable state. Furth quickly realized that the Born criterion also sets the limit of the strength of a perfect crystal subject to external stress that causes deformation strain.[3] Thus, $|C| \to 0$ would be the elastic stability condition at a temperature below melting point when the crystal is under external stress. The Born criterion is formulated for a crystalline solid in a stress-free state, so Furth's generalization is clearly invalid, because the elastic constants at finite deformation depend on applied stress.[4] The Born criterion for crystals in the deformed state should be modified using the stress-dependent elastic constants. The general expression for the elastic constants under an arbitrary applied stress was derived by Wallace in the context of formulating equations of elastic wave propagation in stressed crystals,[4] where he called it the elastic stiffness constant,

$$B_{ijkl} = C_{ijkl} + (1/2)(\delta_{ik}\tau_{jl} + \delta_{jk}\tau_{il} + \delta_{il}\tau_{jk} + \delta_{jl}\tau_{ik} - 2\delta_{kl}\tau_{ij}). \quad (1)$$

Here, $C_{ijkl} = \rho\partial^2 F/\partial\eta_{ij}\partial\eta_{kl}$ is the elastic constant, τ is the applied stress, ρ is the density of the material in a deformed state, and F is the free energy of the system. Using the elastic stiffness constants, the Born stability criterion then becomes

$$|B| > 0. \quad (2)$$

Equation (2) reduces to the original Born criterion at zero applied stress ($\tau = 0$), i.e., $B = C$.

Recently, we[5] showed that the general stability criterion in Eq. (2) is related to the one proposed much earlier by Polanyi, Frenkel, and Orowan[6–8] that predicts the ideal strength of a crystal. The connection is through the relation

$$\tau_{ij}(x) = \tau_{ij}(X) + B_{ijkl}\eta_{kl} + O[(\eta_{kl})^2], \quad (3)$$

where $\tau_{ij}(x)$ is the stress at a current deformed state x away from a reference state X and $\tau_{ij}(X)$ is the stress applied to a system at state X, with η as the Lagrangian strain from state X to state x. If x is sufficiently close to X, the stability criterion is set by

$$\partial\tau/\partial\eta > 0, \quad (4)$$

which is the Frenkel-Orowan criterion.

Using the generalized Born criterion [Eq. (2)], a large number of theoretical and computational work has been performed[9] to investigate the elastic stability problems associated with phase transition, ideal strength, crystal defect formation, etc. A continuum model with a finite element method,[10] an atomistic simulation with an embedded atom method,[11,12] and an *ab initio* quantum mechanic simulation[13–16] have been employed extensively in various calculations. However, all of these approaches require a tremendous amount of computational resources, among which the largest fraction is on calculation of the second-order elastic constant C_{ijkl} in each deformed state. In the *ab initio* calculation, the total energy needs to be calculated first and used later to obtain C_{ijkl}; in the atomistic simulation, C_{ijkl} can be obtained using either an analytical expression or a fluctuation formula.[11,12] For the latter case, a large amount of computation resource is needed to guarantee the convergence of fluctuations so that reliable results can be reached.[17,18] In addition, although the elastic stability criterion as expressed in Eq. (2) is simple, it often hides the physical mechanisms underlying the stability limit. For example, anharmonic effects present in a crystal

under applied stress play an important role in softening the material, leading to elastic instability. By focusing only on the second-order elastic constants C_{ijkl}, this and other effects manifested in higher-order elastic constants are often masked.

In this work, we present a general theoretical framework of the elastic stability criterion using higher-order elastic constants. In finite deformation theory, both the stress and the second-order elastic constants in a stressed state can be expressed in a series expansion in terms of the deformation strain, with the expansion coefficients expressed as functions of stress and the second- and higher-order elastic constants at a reference state. Choosing the reference state as the zero stress state, we obtain the stability criterion as expressed in Eq. (2) in terms of the second- and higher-order elastic constants at zero stress states. Many of these zero stress elastic constants are now available either from experiments or theoretical calculations, making it extremely desirable, and possible, to use the nonlinear formulation analytically to predict the stability and ideal strength of crystalline materials without resorting to extensive computation. In addition, the anharmonic contributions to the elastic stability can be easily seen through the higher-order terms. Another advantage is that we may use this formulation to predict stability conditions at elevated temperatures whenever the elastic constants are available that cannot be easily dealt with using a density functional theory (DFT) calculation, which is confined to zero temperature.

This paper is organized as follows. In Sec. II, we present a unified transcription theory for stress and second- and higher-order elastic constants at different coordinate frames that is needed for our nonlinear theoretical formulation. We express the elastic stability criterion and the nonlinear formulation using second- and higher-order elastic constants at the zero stress state. Instances of the stability criterion for cubic crystals under hydrostatic and uniaxial stress are given. In Sec. III, we present the methods used to test the new theoretical formulations of stability conditions. In Sec. IV, we give the results obtained from several crystalline systems in which higher-order elastic constants are available. They include the stability region expressed by the strain limits, ideal strength or stress, and the possible bifurcation mode of cubic crystal metals, such as Au, Al, Cu, and Si. For comparison, we show results from our *ab initio* calculation and other theoretical works. In Sec. V, we discuss the new method and its applications, along with its limitations, mostly from the view of the quality of the input data. Finally, in Sec. VI, we draw conclusions from this work.

II. THEORY

A. Finite deformation theory of stress and the elastic constant

Suppose a material point in configuration X under stress $\sigma_{ij}(X)$ is undergoing a small displacement, i.e., with a strain η, to a new state x with a corresponding stress $\sigma_{ij}(x)$. We assume, without loss of generality, that the displacement could be arbitrary and infinitesimal as needed. The corresponding change of the Helmholtz free energy $F(x,T) = F(\eta,T)$ at state x from $F(X,T) = F(0,T)$ at state X is expressed as

$$F(\eta,T) = F(0,T) + \left.\frac{\partial F}{\partial \eta_{ij}}\right|_{X,\eta'} \eta_{ij} + \frac{1}{2!}\left.\frac{\partial^2 F}{\partial \eta_{ij}\partial \eta_{kl}}\right|_{X,\eta'} \eta_{ij}\eta_{kl} + \frac{1}{3!}\left.\frac{\partial^3 F}{\partial \eta_{ij}\partial \eta_{kl}\partial \eta_{mn}}\right|_{X,\eta'} \eta_{ij}\eta_{kl}\eta_{mn} + \frac{1}{4!}\left.\frac{\partial^4 F}{\partial \eta_{ij}\partial \eta_{kl}\partial \eta_{mn}\partial \eta_{pq}}\right|_{X,\eta'} \eta_{ij}\eta_{kl}\eta_{mn}\eta_{pq} + \cdots, \tag{5}$$

correct to the fourth order of η with the understanding that all derivatives appearing in Eq. (5) are done at state X with all other strain components η' held constant. The corresponding (second Piola-Kirchhoff) stress and the second-, third-, and higher-order isothermal elastic constants at state X are then

$$\tau_{ij}(X) = \frac{1}{V(X)}\left.\frac{\partial F}{\partial \eta_{ij}}\right|_{X,\eta'}, \tag{6a}$$

$$C_{ijkl}(X) = \frac{1}{V(X)}\left.\frac{\partial^2 F}{\partial \eta_{ij}\partial \eta_{kl}}\right|_{X,\eta'}, \tag{6b}$$

$$c_{ijklmn}(X) = \frac{1}{V(X)}\left.\frac{\partial^3 F}{\partial \eta_{ij}\partial \eta_{kl}\partial \eta_{mn}}\right|_{X,\eta'}, \tag{6c}$$

and

$$\tilde{c}_{ijklmnpq}(X) = \frac{1}{V(X)}\left.\frac{\partial^4 F}{\partial \eta_{ij}\partial \eta_{kl}\partial \eta_{mn}\partial \eta_{pq}}\right|_{X,\eta'}, \tag{6d}$$

where $V(X)$ is the volume of the system at X. Summation convention is automatically assumed.

Following the same scheme, we can obtain the corresponding stress and the second- and third-order isothermal elastic constants at state x as

$$\tau_{ij}(x) = \frac{1}{V(x)}\left.\frac{\partial F}{\partial \xi_{ij}}\right|_{x,\xi'}, \tag{7a}$$

$$C_{ijkl}(x) = \frac{1}{V(x)}\left.\frac{\partial^2 F}{\partial \xi_{ij}\partial \xi_{kl}}\right|_{x,\xi'}, \tag{7b}$$

and

$$c_{ijklmn}(x) = \frac{1}{V(x)}\left.\frac{\partial^3 F}{\partial \xi_{ij}\partial \xi_{kl}\partial \xi_{mn}}\right|_{x,\xi'}, \tag{7c}$$

where $V(x)$ is the volume of the system at state x and ξ is a Lagrangian strain from state x to state y. From the preceding expressions, we can simply take a derivative of Eq. (5) with respect to ξ at state x; thus, we have, after dividing by $V(x)$ on both sides,

$$\tau_{ij}(x) = \frac{1}{V(x)}\left.\frac{\partial F}{\partial \xi_{ij}}\right|_{x,\eta'} = \frac{V(X)}{V(x)}\frac{\partial \eta_{kl}}{\partial \xi_{ij}}\left[\tau_{kl}(X) + C_{klmn}(X)\eta_{mn} + \frac{1}{2!}c_{klmnpq}(X)\eta_{mn}\eta_{pq} + \frac{1}{3!}\tilde{c}_{klmnpqrs}(X)\eta_{mn}\eta_{pq}\eta_{rs} + \cdots\right]. \tag{8a}$$

Following the same scheme, we can systematically obtain the second- and higher-order elastic constants at state x in relation

to those at state X:

$$C_{ijkl}(x) = \frac{1}{V(x)} \left.\frac{\partial^2 F}{\partial\xi_{ij}\partial\xi_{kl}}\right|_{x,\eta'} = \frac{V(X)}{V(x)}\frac{\partial\eta_{mn}}{\partial\xi_{ij}}\frac{\partial\eta_{pq}}{\partial\xi_{kl}} \times \left[C_{mnpq}(X) + c_{mnpqrs}(X)\eta_{rs} + \frac{1}{2!}\tilde{c}_{mnpqrsuv}(X)\eta_{rs}\eta_{uv} + \cdots\right], \quad (8b)$$

$$c_{ijklmn}(x) = \frac{1}{V(x)} \left.\frac{\partial^3 F}{\partial\xi_{ij}\partial\xi_{kl}\partial\xi_{mn}}\right|_{x,\eta'} = \frac{V(X)}{V(x)}\frac{\partial\eta_{pq}}{\partial\xi_{ij}}\frac{\partial\eta_{rs}}{\partial\xi_{kl}}\frac{\partial\eta_{uv}}{\partial\xi_{mn}} \times \left[c_{pqrsuv}(X) + \tilde{c}_{pqrsuvxy}(X)\eta_{xy} + \cdots\right]. \quad (8c)$$

As we show later, these transcription relations enable us to formulate the nonlinear theory of the elastic stability criterion.

B. Elastic stability of crystal solids under external stress

If a material at state X is stable, given a small increment of strain η (with Voigt notation, a strain tensor is treated as a vector, $\eta = (\eta_1,\eta_2,\eta_3,\eta_4,\eta_5,\eta_6)$), the increment of the corresponding stress must remain positive in the direction of the perturbative strain η. Otherwise, the system at state X is unstable. This criterion is what Polanyi, Frenkel, and Orowan[6–8] originally proposed for estimating the ideal strength of a material where $\partial\tau/\partial\eta \to 0$. This approach to obtain stability is effective, because in most calculations and simulations the stress–strain relation can be easily obtained. However, the deformation strain at the instability often does not follow the original loading path. For example,[15] when a face-centered cubic (fcc) crystal Au is under uniaxial tension, the elastic instability is dominated by one of the shear strains rather than the tensile strain. This particular aspect makes it more appealing to use the following approach.

The elastic response coefficient defined in Eq. (1) is often used as a default to judge stability, because the ingredients needed in this criterion can be obtained directly from calculations. It involves τ, the external stress at state X, or the Cauchy stress when the system is in equilibrium, and $C_{ijkl} = V^{-1}(\partial^2 U/\partial\eta_{ij}\partial\eta_{kl})_{\eta=0}$, which is the elastic constant at state X. This stability criterion can be obtained from the convexity of the free energy f of a system under external loading, i.e., $f = F - W$.[5,19–23] With a perturbative strain η, a solid can only be stable when the variation of the internal energy or free energy F is larger than the external work W done to the system, or $\delta(F - W) = \eta^T B\eta > 0$.

Based on its definition, B_{ijkl} is in general asymmetric, while $ij \leftrightarrow kl$ unless the applied stress is hydrostatic $\tau_{ij} \propto \delta_{ij}$. The stability criterion $\delta(F - W) = \eta^T B\eta > 0$ is valid only if the symmetrized part of B, $\overline{B} = (B^T + B)/2$, is positive definite, or $|\overline{B}| > 0$. Specifically, for a cubic crystal subject to hydrostatic pressure P, $\tau_{ij} = -P\delta_{ij}$; thus, $\bar{B} = B$ because of preservation of the lattice symmetry. We follow the convention that the inward pressure is positive while outward one is negative (i.e., $P < 0$ for tension). The stability conditions are

$$B_T(\tau) = (B_{11} + 2B_{12})/3 = (C_{11} + 2C_{12} + P)/3 > 0, \quad (9)$$

$$G'(\tau) = (B_{11} - B_{12})/2 = (C_{11} - C_{12} - 2P)/2 > 0, \quad (10)$$

$$G(\tau) = 4B_{44} = 4(C_{44} - P) > 0. \quad (11)$$

Here, Voigt notation is applied. We express the bulk stiffness modulus $B_T(\tau)$, tetragonal shear stiffness modulus $G\prime(\tau)$, and rhombohedral shear stiffness modulus $G(\tau)$ explicitly.

For a cubic crystal under uniaxial stress along the [100] axis $\tau_{ij} = \tau\delta_{i1}\delta_{j1}$, where $i,j = 1,2,3$, the lattice symmetry becomes tetragonal after deformation. The criterion $|\overline{B}| > 0$ gives four stability conditions, two of which are associated with applied stress explicitly:[24]

$$\overline{B}_{11}(\overline{B}_{22} + \overline{B}_{23}) - 2\overline{B}_{12}^2 > 0$$

$$\Leftrightarrow (C_{11} + \tau)(C_{22} + C_{23}) - 2\left(C_{12} - \frac{\tau}{2}\right)^2 > 0, \quad (12)$$

$$\overline{B}_{22} - \overline{B}_{23} > 0 \Leftrightarrow C_{22} - C_{23} > 0, \quad (13)$$

$$\overline{B}_{44} > 0 \Leftrightarrow C_{44} > 0, \quad (14)$$

$$\overline{B}_{55} > 0 \Leftrightarrow C_{55} + \frac{\tau}{2} > 0. \quad (15)$$

The first condition, in Eq. (12), equals that for the Young's modulus, $E_{100} > 0$. The Young's modulus expressed in terms of the elastic stiffness constants that governs a fully relaxed stretch in the [100] direction is

$$E_{100} = (S_{11})^{-1} = \frac{\overline{B}_{11}(\overline{B}_{22} + \overline{B}_{23}) - 2\overline{B}_{12}^2}{\overline{B}_{22} + \overline{B}_{23}}, \quad (16)$$

where S_{ij} is the elastic compliance tensor for tetragonal crystals.

The ideal tensile or compressive strength of the crystal is the corresponding value of the normal stress τ at which any one of the preceding conditions [Eqs. (12)–(15)] starts to fail. This is different from the original Polanyi-Frenkel-Orowan criterion for theoretical strength mentioned previously, if the strain corresponding to the violation of the stability condition is not along the primary loading path, i.e., in the [100] direction. This phenomenon is called stability bifurcation.[15,16,19–23] The corresponding strain along the primary loading path where any one of the preceding stability conditions is violated sets the strain limit for the materials.

C. Nonlinear theoretical formulation of the elastic stability criterion

As mentioned in the introduction, the necessary ingredient in acquiring the elastic stability criterion expressed in Eq. (2) is the second-order elastic constant C_{ijkl} at the current state, which is usually deformed. To simulate the elastic stability of a crystal solid deformed along a loading path, for each small increment of deformation strain, we must calculate C_{ijkl}, either from the total energy in *ab initio* calculations or from the strain fluctuation in atomistic simulation. This procedure demands a huge computing effort.

Realizing the relations expressed explicitly in Eq. (8) between the stress and the elastic constants at an arbitrary deformed state x and those at a reference state X, we can significantly simplify the procedure to test the elastic stability criterion [Eqs. (1) and (2)] by using a reference state under zero stress, which is often called the natural state in mechanics, where $\tau(X) = 0$. We could express the stress and elastic constants at an arbitrary stressed state x as a function of the deformation strain and the stress and elastic constants at the natural state. We obtain these relations below.

Considering only symmetric strain from X to x, when we use relations $a_{ij} = a_{ji} = \frac{\partial x_i}{\partial X_j}$, $\frac{\partial \eta_{ij}}{\partial \xi_{kl}} = a_{ki}a_{lj}$, the stress in Eq. (8) becomes

$$\tau_{ij} = (V_0/V)a_{ik}a_{jl}\Big[\tau(0)_{kl} + \sum_{mn} C(0)_{klmn}\eta_{mn} + \frac{1}{2}C(0)_{klmnpq}\eta_{mn}\eta_{pq} + \frac{1}{6}C(0)_{klmnpqrs}\eta_{mn}\eta_{pq}\eta_{rs} + \dots\Big], \quad (17)$$

where V_0, $\tau(0)_{kl}$, $C(0)_{klmn}$, $C(0)_{klmnpq}$, and $C(0)_{klmnpqrs}$ represent the volume, the stress, and the second-, third-, and fourth-order elastic constants at the zero stress state, respectively, and V is the volume at the current state x. Similarly, following Eq. (8b), we can write the second-order elastic constants C_{ijkl} at state x as

$$C_{ijkl} = (V_0/V)a_{im}a_{jn}a_{kp}a_{lq}\Big(C(0)_{mnpq} + C(0)_{mnpqrs}\eta_{rs} + \frac{1}{2}C(0)_{mnpqrsuv}\eta_{rs}\eta_{uv} + \cdots\Big). \quad (18)$$

Explicitly, e.g., after using the relations $J = \det|a| = \frac{V(x)}{V(X)} \approx 1 + \eta_{ii} + \cdots$ and $a_{ij} \approx \delta_{ij} + \eta_{ij} - \frac{1}{2}\eta_{ki}\eta_{kj} + \cdots$, Eq. (17) becomes Eq. (3) correct to the first order of η_{ij} (higher-order terms in η_{ij} can also be easily obtained from Eq. (8)), and the second-order elastic constants in Eq. (18) becomes

$$C_{ijkl} = C(0)_{ijkl} + [-C(0)_{ijkl}\eta_{mm} + C(0)_{ijkm}\eta_{lm} + C(0)_{ijml}\eta_{km} + C(0)_{imkl}\eta_{jm} + C(0)_{mjkl}\eta_{im}] + C(0)_{ijklmn}\eta_{mn} + \cdots. \quad (19)$$

Now we have a general expression for τ_{ij} and C_{ijkl} evaluated at any deformed state x in terms of the second-, third-, fourth-, and even higher-order elastic constants evaluated at the zero stress state. If we know these elastic constants, from either experiments or theoretical calculations, we can express the elastic stability conditions analytically, as expressed in Eqs. (9)–(11) or Eqs. (12)–(15), as functions of the deformation strain η only. This new formulation based on the finite deformation theory (Sec. II A) gives significant relief in computing the elastic stability conditions; at the same time, it offers valuable insights into how nonlinear effects such as anharmonicity contribute to crystal stability. In addition, if the data are known, we can also predict stability conditions at elevated temperatures where DFT types of calculations become difficult because they are confined to zero temperature. In the following, we present detailed formulations to implement this approach in cubic crystals.

III. THEORETICAL CALCULATION DETAILS

We performed *ab initio* calculations with DFT to investigate the elastic stability of a fcc crystal Au under hydrostatic and uniaxial stresses, respectively.[15,16] The calculations consist of three parts: (1) equilibrate the system and then subject the system under deformation by applying a homogeneous deformation strain along a specific loading path; (2) obtain the elastic constants, stresses, and other relevant properties, such as volume, at each of the deformed states; and (3) from the elastic constants, obtain the elastic stiffness constants and thus the stability criteria [Eq. (2)]. We can obtain the stability condition using the stress–strain relations [Eq. (3)] too, but caution must be taken in case of a possible occurrence of bifurcation.

In the case of hydrostatic loading, because of the preservation of the symmetry, the procedure is simple. We apply hydrostatic deformation to a crystal supercell via a strain, $\eta_{11} = \eta_{22} = \eta_{33} = \xi$, $\eta_{ij} = 0$ for $i \neq j$, which is done by changing the lattice parameter a homogeneously, or $a/a_0 = \sqrt{1+2\xi}$. We then obtain the pressure–strain relation and the internal energy U as a function of the applied strain, or $U = U(a/a_0)$, from which we obtain the elastic constants.

For uniaxial loading, the procedure is much more complex. To simulate deformation along the [100] axis, we first apply an incremental strain η_1 along the [100] axis to a crystal supercell. We then hold the supercell in the [100] direction but allow it to relax in the other two perpendicular directions, [010] and [001]. When the stress components σ_2 and σ_3 in these two directions reach zero as required by Poisson contraction, we measure the value of η_2 and η_3 and obtain a new supercell, which is now under the nonvanishing stress only along the [100] axis. Because of the tetragonal crystal symmetry and relaxation $\sigma_2 = \sigma_3 = 0$, the total energy of the system is a function of η_1 only. From the total energy of the deformed supercell at each value of η_1, we calculate the elastic constants and test those stability conditions [Eqs. (12)–(15)]. The process is tedious and time consuming. In the following subsections, we present the analytical model using the nonlinear formulation to express the stability conditions for cubic crystals under hydrostatic and uniaxial loadings.

A. Cubic crystals under hydrostatic stress

For a cubic crystal under hydrostatic loading, we have pressure on the system, $\sigma'_{ij} = -P\delta_{ij}$, and the deformation strain $\eta_1 = \eta_2 = \eta_3$. Using Eqs. (17) and (18), we have the pressure and elastic constants for the deformed system in terms of these at zero applied pressure,

$$P = -\frac{1}{3}tr(\sigma') = -\sigma'_1 = \frac{-1}{\sqrt{1+2\eta_1}}[(C_{11}+2C_{12})\eta_1 + \Big(\frac{1}{2}C_{111}+3C_{112}+C_{123}\Big)\eta_1^2 + \Big(\frac{1}{6}C_{1111}+\frac{4}{3}C_{1112} + C_{1122}+2C_{1123}\Big)\eta_1^3] + \cdots, \quad (20)$$

correct to the third order of the Lagrangian strain, and

$$C'_{11} = \sqrt{1+2\eta_1}\big[C_{11} + (C_{111}+2C_{112})\eta_1 + \big(\tfrac{1}{2}C_{1111}+2C_{1112}+C_{1122}+C_{1123}\big)\eta_1^2\big], \quad (21a)$$

$$C'_{12} = \sqrt{1+2\eta_1}\big[C_{12} + (2C_{112} + C_{123})\eta_1 + \big(C_{1112} + C_{1122} + \tfrac{5}{2}C_{1123}\big)\eta_1^2\big], \quad (21b)$$

and

$$C'_{44} = \sqrt{1+2\eta_1}\big[C_{44} + (C_{144} + 2C_{155})\eta_1 + \big(\tfrac{1}{2}C_{1144} + C_{1155} + 2C_{1255} + C_{1266}\big)\eta_1^2\big], \quad (21c)$$

correct to the second order of the Lagrangian strain. Using these relations, we can test the stability conditions expressed in Eqs. (9)–(11).

B. Cubic crystals under uniaxial stress along the [100] axis

We denote the original state by X, i.e., corresponding to an initial state of a cubic supercell (not necessarily the natural or stress-free state); the state with applied strain η_1 by X'; and the state after relaxation by X'', where the latter two states are with tetragonal symmetry. Then, from X to X'', using Eq. (17), we have the stress

$$\begin{aligned}\sigma_1'' &= \frac{1}{V''}\left(\frac{\partial U}{\partial \eta_1''}\right) = \frac{V_0}{V''}\left(\frac{1}{V_0}\frac{\partial U}{\partial \eta_1}\right)\left(\frac{\partial \eta_1''}{\partial \eta_1}\right)\\ &= \frac{\sqrt{1+2\eta_1}}{1+2\eta_2}\Big[\sigma_1 + C_{11}\eta_1 + C_{12}(\eta_2+\eta_3) + \frac{1}{2}C_{111}\eta_1^2\\ &\quad + C_{112}\eta_1(\eta_2+\eta_3) + \frac{1}{2}C_{112}\big(\eta_2^2+\eta_3^2\big) + C_{123}\eta_2\eta_3\\ &\quad + \frac{1}{6}C_{1111}\eta_1^3 + \frac{1}{2}C_{1112}\eta_1^2(\eta_2+\eta_3) + \frac{1}{6}C_{1112}\big(\eta_2^3+\eta_3^3\big)\\ &\quad + \frac{1}{2}C_{1122}\eta_1\big(\eta_2^2+\eta_3^2\big) + C_{1123}(\eta_1\eta_2\eta_3\\ &\quad + \frac{1}{2}\eta_2^2\eta_3 + \frac{1}{2}\eta_2\eta_3^2)\Big], \end{aligned} \quad (22)$$

correct to the third order of Lagrangian strain. We now choose state X as the natural state, $\sigma_1 = 0$. Similarly, we may use Eq. (18) to have the six independent second-order elastic constants at state X'',

$$C''_{11} = \frac{(1+2\eta_1)^{3/2}}{(1+2\eta_2)}\Big[C_{11} + C_{111}\eta_1 + C_{112}(\eta_2+\eta_3) + \frac{1}{2}C_{1111}\eta_1^2 + C_{1112}\eta_1(\eta_2+\eta_3) + \frac{1}{2}C_{1122}\big(\eta_2^2+\eta_3^2\big) + C_{1123}\eta_2\eta_3\Big], \quad (23a)$$

$$C''_{22} = \frac{(1+2\eta_2)}{(1+2\eta_1)^{1/2}}\Big[C_{11} + C_{111}\eta_2 + C_{112}(\eta_1+\eta_3) + \frac{1}{2}C_{1111}\eta_2^2 + C_{1112}\eta_2(\eta_1+\eta_3) + \frac{1}{2}C_{1122}\big(\eta_1^2+\eta_3^2\big) + C_{1123}\eta_1\eta_3\Big], \quad (23b)$$

$$C''_{12} = (1+2\eta_1)^{1/2}\Big[C_{12} + C_{112}(\eta_1+\eta_2) + C_{123}\eta_3 + \frac{1}{2}C_{1112}\big(\eta_1^2+\eta_2^2\big) + C_{1122}\eta_1\eta_2 + C_{1123}(\eta_1\eta_3 + \eta_2\eta_3 + \frac{1}{2}\eta_3^2)\Big], \quad (23c)$$

$$C''_{23} = \frac{(1+2\eta_2)}{(1+2\eta_1)^{1/2}}\Big[C_{12} + C_{112}(\eta_2+\eta_3) + C_{123}\eta_1 + \frac{1}{2}C_{1112}\big(\eta_2^2+\eta_3^2\big) + C_{1122}\eta_2\eta_3 + \frac{1}{2}C_{1123}\big(\eta_1^2 + 2\eta_1\eta_2 + 2\eta_1\eta_3\big)\Big], \quad (23d)$$

$$C''_{44} = \frac{(1+2\eta_2)}{(1+2\eta_1)^{1/2}}\Big[C_{44} + C_{144}\eta_1 + C_{155}(\eta_2+\eta_3) + \frac{1}{2}C_{1144}\eta_1^2 + \frac{1}{2}C_{1155}\big(\eta_3^2+\eta_2^2\big) + C_{1255}(\eta_1\eta_2 + \eta_1\eta_3) + C_{1266}\eta_2\eta_3\Big], \quad (23e)$$

and

$$C''_{55} = (1+2\eta_1)^{1/2}\Big[C_{44} + C_{144}\eta_2 + C_{155}(\eta_1+\eta_3) + \frac{1}{2}C_{1144}\eta_2^2 + \frac{1}{2}C_{1155}\Big(\eta_3^2+\eta_1^2\Big) + C_{1255}(\eta_1\eta_2 + \eta_2\eta_3) + C_{1266}\eta_1\eta_3\Big], \quad (23f)$$

correct to the second order of the Lagrangian strain. With Eqs. (22) and (23), we have the stress and elastic constants at state X'' all expressed in terms of η_1 and the second-, third-, and fourth-order elastic constants at state X, given the condition that $\eta_2 = \eta_3 = f(\eta_1)$ as required from $\sigma_2'' = \sigma_3'' = 0$ after relaxation from state X'. To identify the value of η_2 and η_3 for each specific η_1, we use the procedure given in the appendix. Therefore, using the available elastic constants at zero stress, we can test the stability conditions expressed in Eqs. (12)–(15) involving the stress and elastic constants at any deformed state X''.

IV. RESULTS

In the following, we present the results on testing the nonlinear formulation of the elastic stability conditions expressed in two forms, one in terms of the elastic stiffness coefficients [Eq. (2)] and the other from the stress–strain relation [Eq. (3)]. In the nonlinear formulation, both the stress and the elastic constants are functions of the deformation strain only. The inputs are the second-, third-, and fourth-order elastic constants at a natural state from available experimental measurements or theoretical calculations. The quality of the input data has

a big effect on the stability results, especially at large strains. We discuss this issue in more detail in the next section. For comparison, we also use the results from *ab initio* calculations and atomistic simulations, in particular those from our own DFT calculation of Au, where all elastic constants up to the fourth order were available in our previous publication.[25]

A. Fcc crystal Au under hydrostatic stress

Figure 1 gives the stress–strain curves of both analytical results and *ab initio* calculations for the crystal Au under hydrostatic stress. We have two stress–strain curves from Eq. (20), resulting from two sets of data of the elastic constants, one from the experiments[26] and the other from our recent *ab initio* calculations.[25] The analytical results agree well with those from the DFT calculation in the presented large strain range, and the one with experimental input deviates from the other two only in the compressive regime.

Figures 2(a)–2(c) shows the elastic stiffness moduli defined in Eqs. (9)–(11) with varying hydrostatic strains. As for the stress–strain relation, three sets of results are obtained for each stiffness modulus. When we use the second-, third-, and fourth-order elastic constants of the stress-free crystal Au from our calculations and the experiments, the results agree well with the direct *ab initio*–calculated stiffness moduli. Our earlier *ab initio* calculation work[15] shows that under hydrostatic stress, the instability does not occur along the primary volumetric deformation path; instead, it happens along a bifurcated path, the rhombohedral shear path at the expansion strain of 0.06.[15] The analytical results using the elastic constants from our *ab initio* calculations show that under compression, all three stability conditions [Eqs. (9)–(11)] are obeyed within a 10% strain range. In expansion, the stability conditions associated with the bulk and tetragonal shear stiffness moduli [Eqs. (9) and (10)] are maintained [Figs. 2(a) and 2(b)], and the rhombohedral shear stiffness condition is violated; i.e., it goes to zero first at the Lagrangian strain $\eta_1 \sim 0.05$, which agrees well with our previous direct *ab initio* calculation of the stability condition [Fig. 2(c)].[15]

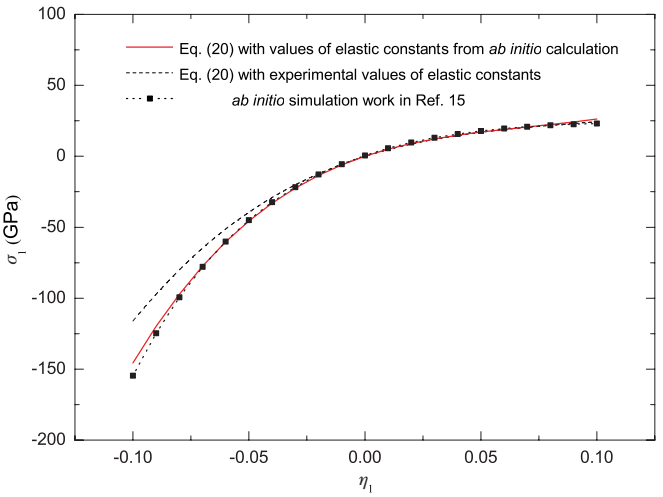

FIG. 1. (Color online) Hydrostatic stress varies with strain η_1 for a fcc crystal Au. Two of the stress–strain curves use Eq. (20), with two sets of data for the elastic constants in the nonlinear theoretical formulation, one from experiments and the other from our recent *ab initio* calculation. The third curve comes from our *ab initio* calculation.

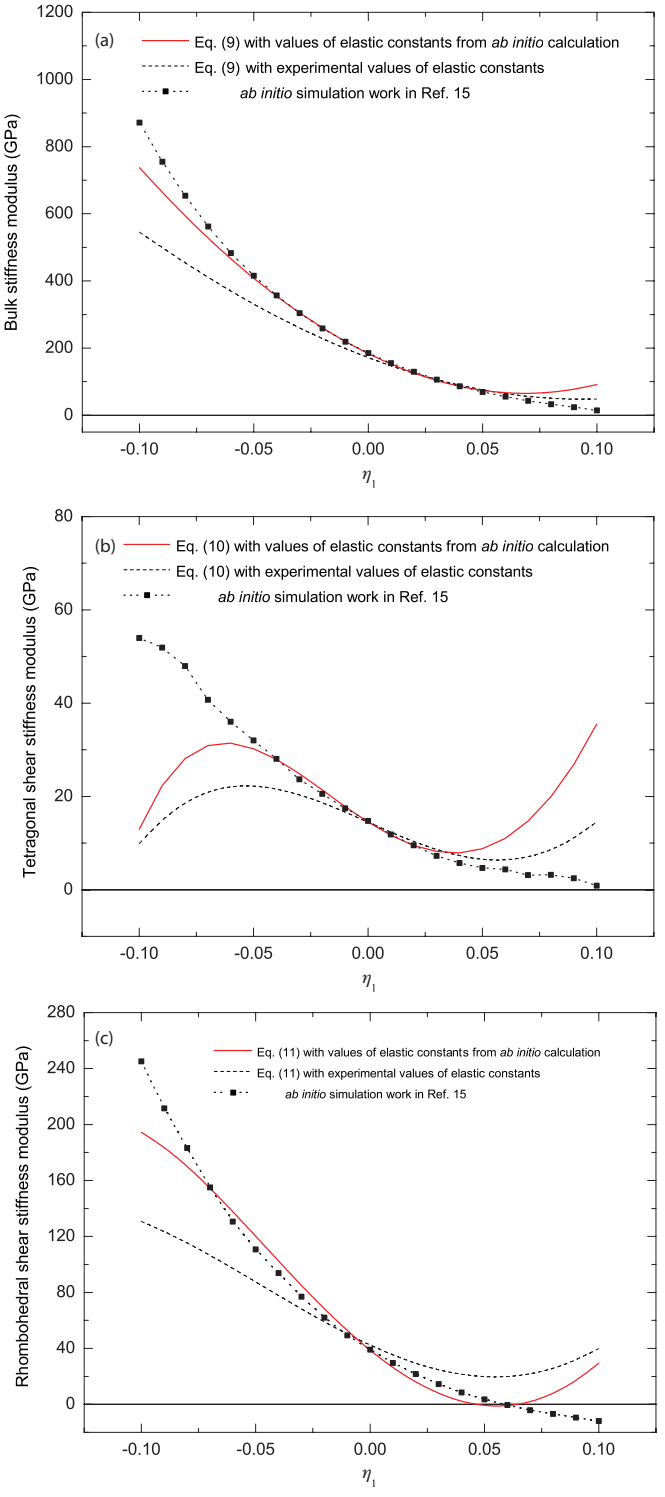

FIG. 2. (Color online) Three elastic moduli of Au under hydrostatic deformation versus volume strain η_1: (a) bulk stiffness constants, (b) tetragonal shear stiffness constants, and (c) rhombohedral shear stiffness constants. Under compression, the crystal is stable. While under expansion, the rhombohedral shear stiffness modulus reaches zero first at $\eta_1 \sim 0.05$.

The rhombohedral shear stiffness condition from the analytical result using the experimental elastic constants does not show instability, although a minimum at the same strain ($\eta_1 \sim 0.05$) can be seen. Moreover, the rhombohedral shear stiffness modulus increases at the large strain, mainly because of the use of the fourth-order elastic constants, while that from the direct *ab initio* calculation shows a monotonous decrease with volume expansion.

As we mentioned previously, the rhombohedral shear instability showing up as instability bifurcation cannot be captured directly from the hydrostatic pressure–strain curves, as shown in Fig. 1. Accordingly, the theoretical strength cannot be obtained from the pressure–strain curve using the Frenkel-Orowan criterion. Instead, it can only be obtained from information about the shear instability from the generalized Born criterion. From the analytical stress–strain curves (Fig. 1), using the input elastic constants from our previous *ab initio* calculations, we obtain the ideal hydrostatic strength of 17.1 GPa that corresponds to the shear instability at $\eta_1 \sim 0.05$. As a comparison, it is 19.2 GPa from direct *ab initio* calculations.[15]

B. Diamond-structure Si under hydrostatic stress

Karki *et al.*[27] employed *ab initio* calculations to test the stability conditions of diamond-structure Si under hydrostatic pressure. Their results show that the tetragonal shear modulus decreases with pressure and vanishes ∼101 GPa, while rhombohedral shear modulus decreases to zero at a higher pressure of 107 GPa. We used the fourth-order elastic constants obtained by Gerlich *et al.*[28] with Keating model to test the elastic stability of Si with the preceding nonlinear theoretical formulation. We found that the tetragonal shear modulus approaches zero under pressure at 69 GPa, while the rhombohedral shear modulus decreases to zero at 32 GPa. In Gerlich's work, the errors in the fourth-order elastic constants

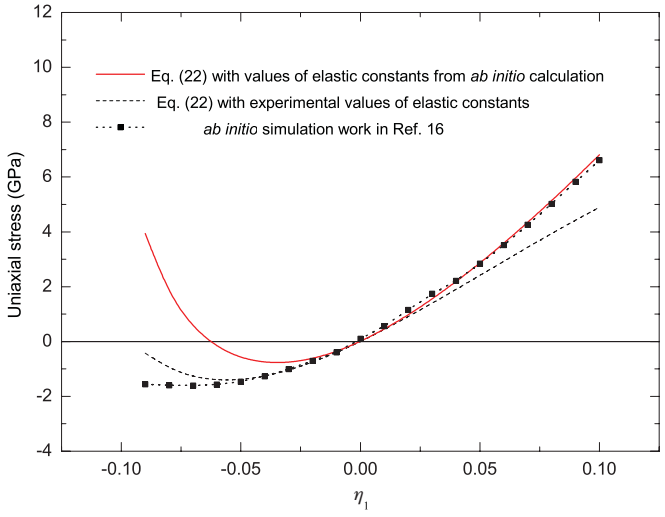

FIG. 3. (Color online) Normal stress varies with strain η_1 when an fcc crystal Au is under uniaxial stress in the [100] direction. Two of the stress–strain curves come from Eq. (22), with two sets of data for the elastic constants in the nonlinear theoretical formulation: one from experiments and the other from our recent *ab initio* calculations. The stress–strain curve from our *ab initio* calculation is also shown.

are more than even 100%, which might be the major reason we cannot use those elastic constants to obtain satisfactory results.

C. Fcc crystal Au under uniaxial stress along the [100] axis

As compared with the hydrostatic case, uniaxial loading is more complicated because of symmetry breaking. Figure 3 gives uniaxial stress as a function of strain η_1 in the [100] direction for a fcc crystal Au under uniaxial stress (tension and compression). Three sets of results are presented: one is from the direct *ab initio* calculation, and the other two are from Eq. (22) using the elastic constants from experiments[26] and our DFT calculations.[25] The three lines agree well with one another in the range of small strains of less than 0.02. Beyond this range, some differences occur. In general, the analytical result using the elastic constants calculated from the *ab initio* results agrees well with the stress–strain relation obtained directly from *ab initio* calculation, but the analytical result using the experimental data differs substantially from the *ab initio* ones, which is understandable considering that the experimental data were not obtained at zero temperature. Instead, they came from different measurements with approximations, noticeably using the Cauchy relation.[26] Another obvious deviation among the stress–strain relations occurs at larger strains in the compression region. The analytical result using the elastic constants from the DFT calculations shows a larger deviation from the direct *ab initio* calculation result. Those deviations occur partly because only a finite number of terms are kept in the deformation energy up to the fourth order in strain η_1. Nevertheless, as shown later, the deviation in stress–strain relations does not affect the prediction of the stability conditions.

Using the relations in Eq. (23), we obtained the elastic constants at a deformed state, from which we can obtain the stiffness constants [Eq. (1)] and thus test the stability criteria for Au under uniaxial loading [Eqs. (12)–(15)]. Figures 4(a)–4(d) gives these elastic stiffness moduli as functions of η_1. In general, the trend in each of the four moduli as functions of uniaxial strain is captured well by the analytical results as compared with the direct *ab initio* calculations, although increasing deviation occurs at larger strains because of the use of only finite terms in the theory. The most salient feature is that nonlinear theory can predict instability and bifurcation relatively well (within the range of the strains before large deviation from these of *ab initio* calculation occurs). As shown in Fig. 4(a), under tensile stress, the stability condition involving the tetragonal shear modulus [Eq. (13)] is violated first. The corresponding Lagrangian strain is at $\eta_1 \sim 0.048$, where the shear stiffness modulus calculated using the elastic constants from the *ab initio* calculations vanishes, and at $\eta_1 \sim 0.10$, where the shear stiffness modulus calculated using the experimental input data for elastic constants vanishes. Again, the instability occurs not along the primary loading strain path but along a shear path, via instability bifurcation, which is well captured by the theory. Figs. 4(b) and 4(c) shows that there is no instability triggered by two other shear stiffness coefficients; both $\bar{B}_{44}$ and $\bar{B}_{55}$ remain finite within the range of strains before the tetragonal shear instability occurs.

As shown in Fig. 4(d), under compression, the stability condition governed by the Young's stiffness modulus [Eq. (12)

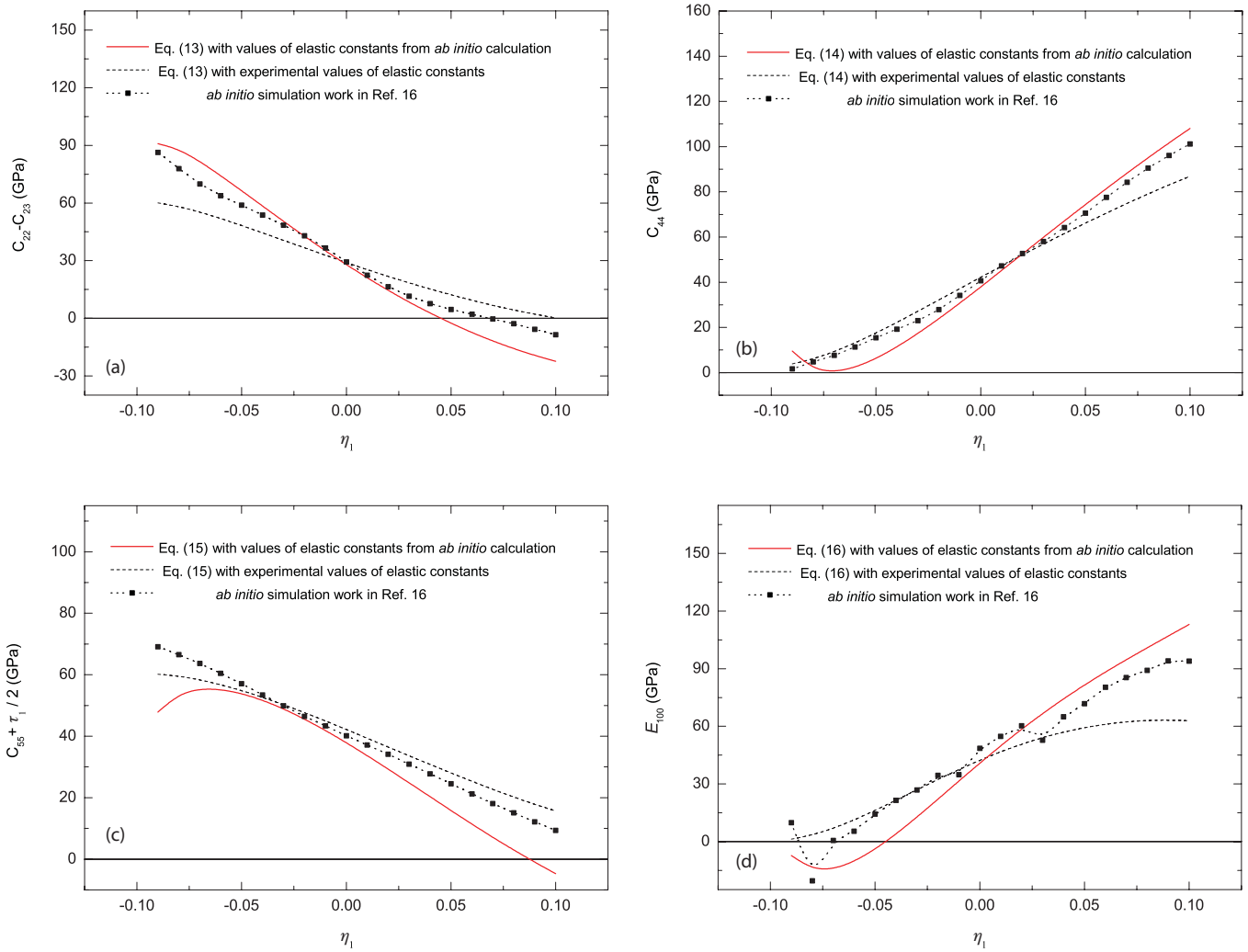

FIG. 4. (Color online) Four elastic stiffness moduli of Au under uniaxial stress varying with uniaxial strain η_1. Under compression, the Young's modulus reaches zero first at $\eta_1 \sim -0.045$; under tensile stress, the tetragonal shear stiffness modulus reaches zero first at $\eta_1 \sim 0.048$.

or (16)] is violated first at the Lagrangian strains $\eta_1 \sim -0.045$ and $\eta_1 \sim -0.085$ using the input elastic constants from the *ab initio* calculations and experiments, respectively. As a comparison, the corresponding strain limits at these tension and compression instability points from our previous *ab initio* calculation are 0.07 and −0.07, respectively.[16]

Given the stress–strain curve (Fig. 3), from nonlinear theory with inputs from the *ab initio* calculation, we can locate the ideal tensile strength of Au, which is 2.7 GPa at the shear instability point $\eta_1 \sim 0.048$, and the ideal compressive strength, which is 0.7 GPa at the compressive strain of $\eta_1 \sim -0.045$. The strengths predicted from the shear–strain bifurcation are much smaller than the ideal strengths at the instability points at $\eta_1 \sim -0.085$ and $\eta_1 \sim 0.10$ predicted using experimental measurements of elastic constants.

D. Other fcc crystals

The cases of Au presented previously are unique: the required input elastic constants up to the fourth order are available from both theoretical calculations and experiments, and the direct *ab initio* simulations of both hydrostatic and uniaxial deformation modes are available for comparison.[15,16] In a recent work, we calculated the elastic constants of several fcc metals up to the fourth order.[25] This effort makes it possible to extend the nonlinear formulation of elastic stability to those materials, including Al and Cu. Because detailed approaches have been given in the last two sections, we only summarize the results for these fcc crystals subject to hydrostatic and uniaxial loading (Table I). Our emphasis is on the elastic stability from the nonlinear formulation, the ideal strength and strain, and the stability mode under which the stability condition is violated.

The ideal strength and stable region of strain are obtained using the new formulation for Au, Al, and Cu under uniaxial tension and compression in the [100] direction. Table I lists the results from our nonlinear analytical theory, previous *ab initio* calculation work,[13,14,16] and embedded atom method.[11,12] As in Au, the maximum tensile strength for Al and Cu is determined by shear bifurcation via tetragonal shear instability, where $\bar{B}_{22} - \bar{B}_{23} = 0$, and the maximum compressive strength is determined by tensile instability at a vanishing Young's

TABLE I. The ideal strength and stable region of fcc crystals Au, Al, and Cu under uniaxial stress along the [100] axis. The results are from our analytical scheme, our *ab initio* calculation, and the embedded atom method.

	Tension $C_{11} - C_{12} = 0$		Compression $E_{[100]} = 0$	
	σ_1 (GPa)	η_1	σ_1 (GPa)	η_1
Au	2.7[a]	0.048[a]	−0.7[a]	−0.045[a]
	4.2[b]	0.07[b]	−1.6[b]	−0.07[b]
	6.31[c]	0.079[c]	−2.21[c]	−0.098[c]
	10.0[f]	0.11[f]	–	–
Al	6.7[a]	0.11[a]	−5.8[a]	−0.09[a]
	12.1[d]	0.27[d]	−5.62[d]	−0.10[d]
	11.1[f]	0.25[f]	–	–
Cu	8.2[a]	0.09[a]	−2.6[a]	−0.08[a]
	9.4[e]	0.10[e]	−3.5[e]	−0.09[e]
	9.8[f]	0.14[f]	–	–

[a]This work.
[b]Reference 16.
[c]Reference 12.
[d]Reference 13.
[e]Reference 14.
[f]Reference 11.

stiffness coefficient, i.e., E_{100}. Depending on the method used, the numerical values of the maximum strengths and the strains corresponding to the maximum strength under tension and compression vary widely for the same system. For example, for Au, the tensile maximum strength is 2.7, 4.2, 6.31, and 10.0 GPa and the corresponding strain limit is 0.048, 0.07, 0.079, and 0.11, respectively. In general, the molecular dynamics simulation gives the highest strength and largest limiting strain, whereas the nonlinear elastic theory has the smallest strength and smallest strain. The agreement between these methods is the remarkably consistent prediction of the mode under which the instability occurs. For example, all fcc metals have tensile strength determined by tetragonal shear bifurcation, and compression strength is determined by instability in the Young's stiffness coefficient.

V. DISCUSSION

The results shown previously indicate that our analytical model gives similar results with the ones from our *ab initio* calculations in terms of the deformation mode at instability and even the values of theoretical strength and strain. This is not surprising, because the elastic constants used in the nonlinear theory are from the same *ab initio* calculations. Larger deviation occurs between these results and those using experimental elastic constants. The difference may come from a few sources. First, the elastic constants are calculated at zero temperature using the *ab initio* method, while the experimental ones are usually at room temperature. A 20%–30% change in the elastic stiffness constants at different temperatures, such as in the case of tetragonal shear instability $\bar{B}_{22} - \bar{B}_{23}$, can lead to the difference in the limiting strains and the maximum strength. Second, when we calculate those second-, third-, and fourth-order elastic constants,[25] we apply small perturbative strains to the supercell to get the energy–strain curve. The elastic constants are obtained by fitting the energy–strain curves.

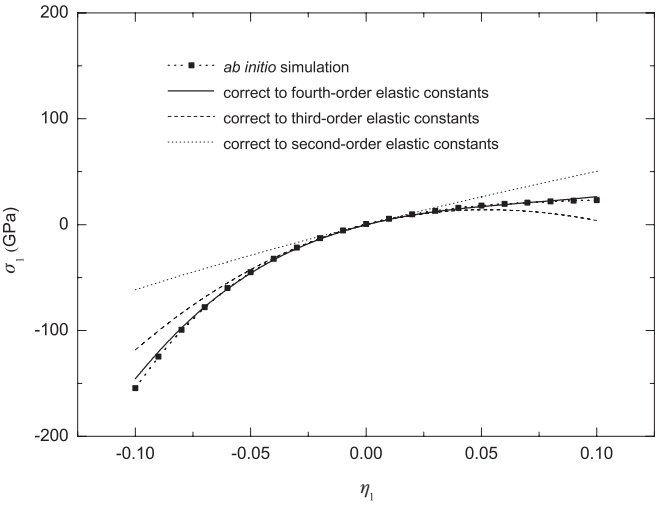

FIG. 5. Equation of state calculated for Au using various truncated terms in Eq. (20) to the second-, third-, and fourth-order elastic constants. As a comparison, the stress–strain curve from our *ab initio* calculation is also shown.

Therefore, system errors occur and propagate during these procedures when we apply the stress and elastic constants in Eqs. (20)–(23). Third, our *ab initio* work[16] employs the stress–strain relation to obtain elastic moduli, which is different from the energy–strain method we use to obtain the elastic constants. Therefore, we may find in Fig. 4 that, at the original size of the supercell, the modulius values obtained from these two methods are not exactly the same. For these reasons, we do not expect the curves from the analytical method and those from the *ab initio* calculations to overlap completely in Fig. 4.

In Figs. 1–4, we also give analytical results using experimental values of second-, third-, and fourth-order elastic constants of Au. The second- and third-order elastic constants were measured at room temperature using high-purity single crystals.[26] Based on those values, Hiki *et al.*[29] estimated the fourth-order elastic constants with the generalized Cauchy relationship:

$$C_{1111} = 2C_{1112} = 2C_{1122} = 2C_{1155} = 2C_{1266} = 2C_{4444},$$
$$C_{1123} = C_{1144} = C_{1255} = C_{1456} = C_{4455} = 0.$$

This is a quite rough approximation. However, the fourth-order elastic constants that Hiki *et al.* got are the only set of data we can find, because no experimental data of fourth-order elastic constants are available to date. When we use Hiki *et al.*'s fourth-order elastic constants of Au, the analytical scheme gives somewhat different results from those obtained using our own *ab initio*–calculated elastic constants.

Different from the uncertainties in our approaches presented previously, there are various sources of uncertainties in other theoretical and simulation approaches. These different sources of uncertainties contribute to the differences in the results shown in Table I. For example, Milstein *et al.*[11] used an embedded atom method to perform simulation. Their potentials are quite sophisticated, because they are fitted to the second- and third-order elastic constants. However, according our experience, at such a large finite strain range, which is beyond 0.10, the fourth-order elastic constants would make contributions and must be taken into account in the

fitting procedures of the potentials.[25] Perhaps because of that, their values of ideal tensile strength are higher, and the stable range in tension is wider than ours. Zhang *et al.*[12] employed a modified analytical embedded atom method model to investigate the same problem. Their results are closer to ours. Li and Wang[13] studied the ideal strength of Al, but they did not use symmetrized elastic stiffness constants. In addition, how they calculate each elastic constant at a given stressed state to test the stability conditions is not clear. Cerny *et al.*[14] worked on the ideal strength of Cu, but the Young's modulus formulation they used is valid only in a small deformation.[16] Recently, Cerny and Pokluda[30] presented another way to estimate uniaxial tensile strength on the basis of theoretical shear strength calculations. They claimed that the analysis of elastic stability of crystals under tensile loading would be avoided using this method. Their work shows that the ideal tensile strength is 5.8 GPa from the rigid-planes approach and 3.6 GPa from the relaxed-planes approach.

Krenn *et al.*[31] applied the transcription theory of stress and elastic constants to the nonlinear elastic behavior of the fcc crystals Al and Cu. They used experimentally measured second- and third-order elastic constants to explain the different structural relaxation modes of the crystals Al and Cu under shear deformation. Partly because of the inaccuracy of the experimental data but more importantly because of the limitation of the third-order elastic constants, their work gives only correct signs of relaxations along the x, y, and z axes, not the magnitudes. At a finite strain range of $\sim$10%, the fourth-order elastic constants play an essential role in the transcription theory scheme.

Perhaps the most obvious discrepancy comes from the truncation of the higher-order terms involving fourth- and higher-order elastic constants. We demonstrate the case through Eq. (20) for the hydrostatic stress that is expressed at the second-, third-, and fourth-order elastic constants. The stress–strain curve in Fig. 5 shows the increasing accuracy of the stress–strain relation as compared with our *ab initio*–calculated curve. We also checked the relation in Eq. (21) at various truncations. Figure 6 shows the bulk stiffness modulus with different orders of accuracy varying with strain η_1. Figures 5 and 6 give us a general idea that when the analytical scheme is correct to the fourth-order elastic constants, the results usually come to fairly good agreement with the results from *ab initio* calculations, at least within the strain range where elastic instability occurs.

The calculations performed in this work are based on the concept of elastic stability, which corresponds to the long-wave phonon limit. Some soft phonon modes, most likely those along the rhombohedral or tetragonal shear, may appear in the hydrostatically deformed crystal. Recent studies on elastic[13] and phonon[32] instabilities of aluminum suggest that this scenario may likely occur in fcc metals, especially at elevated temperatures.

VI. CONCLUSION

The current methods of accessing the elastic instability and the related theoretical strength and strain are either through the Frenkel-Orowan model [Eq. (3)] using direct computation of the stress–strain relation or via the generalized Born criterion

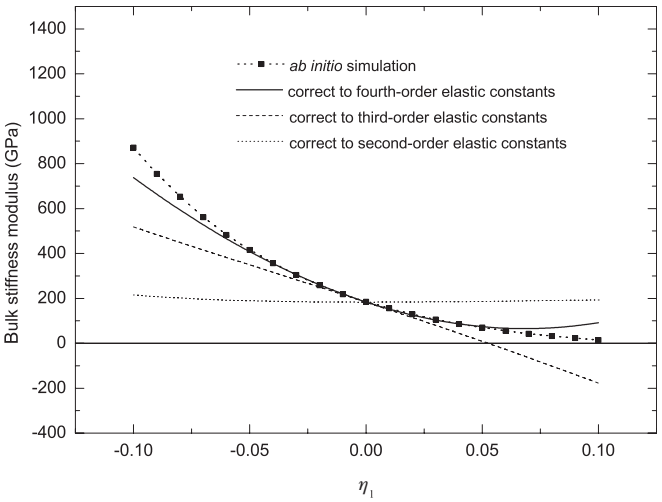

FIG. 6. The bulk stiffnessmodulus obtained with Eq. (9) by using Eqs. (20) and (21) with the second-, third-, and fourth-order elastic constants. For comparison, the modulus–strain relation from our *ab initio* calculation is also shown.

using the stiffness coefficient B. The drawback of the former is its inability to predict elastic instability bifurcation that happens before the maximum strength and strain are reached along the original loading path, and that of the latter is the requirement of extensive computation to obtain the second-order elastic constants at each deformed state to furnish B [Eq. (1)]. In addition, some critical physical effects such as anharmonicity are masked in this formulation. In this work, we developed a general nonlinear theoretical formulation to overcome these limitations. The theory utilizes the high-order elastic constants at the zero stress state, or those at any deformed state that are available either in experiment or through *ab initio* calculation or atomistic simulation. We tested the theory in several cubic crystals, including Au, Al, Cu, and Si, using available data. The stable region, ideal strength, and limiting strains were obtained and found to be in good agreement with *ab initio* calculations in locating the mode of instability. The analytical scheme gives us a new and computationally efficient way to investigate ideal strength, bifurcation, and elastic stability problems in solids. Another advantage is that we may be able to use the theory for solids at elevated temperatures where DFT types of calculations may not be usable.

ACKNOWLEDGMENTS

The authors are grateful for the financial support of this work provided by the by the NSF under the Contract No. NSF-0907320.

APPENDIX

From state X' to state X'', the internal energy as a function of strain η', expanded to $O(\eta'^3)$, may be written as

$$\delta U' = \sum_i \sigma_i' \eta_i' + \frac{1}{2} C_{11}' \eta_1'^2 + \frac{1}{2} C_{22}' \left(\eta_2'^2 + \eta_3'^2\right) + C_{12}' (\eta_1' \eta_2' + \eta_3' \eta_1') + C_{23}' \eta_2' \eta_3' + \frac{1}{6} C_{111}' \eta_1'^3$$

$$+\frac{1}{6}C'_{222}\left(\eta_2'^3+\eta_3'^3\right)+\frac{1}{2}\Big[C'_{112}\eta_1'^2(\eta_2'+\eta_3') + C'_{122}\eta_1'\left(\eta_2'^2+\eta_3'^2\right)+C'_{223}\eta_2'\eta_3'(\eta_2'+\eta_3')\Big] + C'_{123}\eta_1'\eta_2'\eta_3', \quad \text{(A1)}$$

where σ_i', C'_{ij}, and C'_{ijk} represent the stress and elastic constants at state X' and η_i' represents the Lagrangian strain from state X' to state X''. We know that $\eta_2'=\eta_3'$, $\eta_1'=0$, and $\sigma_2'=\sigma_3'$. Let σ_i'' represent the stress at state X'', $\sigma_2''=\sigma_3''=0$. With Eq. (8a), we have

$$\sigma_2''=\sigma_2'+C'_{22}\eta_2'+C'_{23}\eta_3'+\tfrac{1}{2}C'_{222}\eta_2'^2+\tfrac{1}{2}C'_{223}\left(2\eta_2'\eta_3'+\eta_3'^2\right). \quad \text{(A2)}$$

Using $\sigma_2''=0$, $\eta_2'=\eta_3'$,

$$0=\sigma_2'+(C'_{22}+C'_{23})\eta_2'+\left(\tfrac{1}{2}C'_{222}+\tfrac{3}{2}C'_{223}\right)\eta_2'^2. \quad \text{(A3)}$$

To solve this equation, we need to know the values of σ_2', C'_{22}, C'_{23}, C'_{222}, and C'_{223}.

From state X to state X', $\eta_i=0$ $(i\neq 1)$, $\frac{V}{V'}=\frac{1}{\sqrt{1+2\eta_1}}$. Again, we use Eqs. (8a)–(8c) and have

$$\sigma_2'=\frac{1}{\sqrt{1+2\eta_1}}\left(C_{12}\eta_1+\frac{1}{2}C_{112}\eta_1^2+\frac{1}{6}C_{1112}\eta_1^3\right), \quad \text{(A4)}$$

$$C'_{22}=\frac{1}{V'}\frac{\partial^2U}{\partial\eta_2'^2}=\left(\frac{V}{V'}\right)\left(\frac{1}{V}\frac{\partial^2U}{\partial\eta_2^2}\right)a_{22}^4 = \frac{1}{\sqrt{1+2\eta_1}}\left[C_{11}+C_{112}\eta_1+\frac{1}{2}C_{1122}\eta_1^2\right], \quad \text{(A5)}$$

$$C'_{23}=\frac{1}{V'}\frac{\partial^2U}{\partial\eta_2'\partial\eta_3'}=\left(\frac{V}{V'}\right)\left(\frac{1}{V}\frac{\partial^2U}{\partial\eta_2\partial\eta_3}\right)a_{22}^2a_{33}^2 = \frac{1}{\sqrt{1+2\eta_1}}\left[C_{12}+C_{123}\eta_1+\frac{1}{2}C_{1123}\eta_1^2\right], \quad \text{(A6)}$$

$$C'_{222}=\frac{1}{V'}\frac{\partial^3U}{\partial\eta_2'^3}=\left(\frac{V}{V'}\right)\left(\frac{1}{V}\frac{\partial^2U}{\partial\eta_2^3}\right)a_{22}^6 = \frac{1}{\sqrt{1+2\eta_1}}[C_{111}+C_{1112}\eta_1], \quad \text{(A7)}$$

$$C'_{223}=\frac{1}{V'}\frac{\partial^3U}{\partial\eta_2'^2\partial\eta_3'}=\left(\frac{V}{V'}\right)\left(\frac{1}{V}\frac{\partial^3U}{\partial\eta_2^2\partial\eta_3}\right)a_{22}^4a_{33}^2 = \frac{1}{\sqrt{1+2\eta_1}}[C_{112}+C_{1123}\eta_1]. \quad \text{(A8)}$$

Here, all coefficients in Eq. (A3) are expressed in terms of η_1,C_{ij}, C_{ijk}, and C_{ijkl}. We get a solution of η_2 from Eq. (A3) for an arbitrary value of η_1.

*mo.li@mse.gatech.edu

[1] M. Born, Math. Proc. Camb. Phil. Soc. **36**, 160 (1940).
[2] M. Born, J. Chem. Phys. **7**, 591 (1939).
[3] R. Furth and M. Born, Nature **145**, 741 (1940).
[4] D. C. Wallace, *Thermodynamics of Crystals* (Dover Publications, Mineola, New York, 1998).
[5] H. Wang and M. Li, unpublished results.
[6] M. Polanyi, Z. Phys. **7**, 323 (1921).
[7] J. Frenkel, Z. Phys. **37**, 572 (1926).
[8] E. Orowan, Rep. Prog. Phys. **12**, 183 (1948).
[9] M. Sob, M. Friak, D. Legut, and V. Vitek, Mater. Sci. Eng. A **148**, 387 (2004).
[10] X. Liu, Z. Liu, X. You, J. Nie, and Z. Zhuang, Chin. Phys. Lett. **26**, 026103 (2009).
[11] F. Milstein and S. Chantasiriwan, Phys. Rev. B **58**, 6006 (1998).
[12] J. Zhang, Y. Yang, and K. Xu, Can. J. Phys. **86**, 935 (2008).
[13] W. X. Li and T. C. Wang, J. Phys. Condens. Matter **10**, 9889 (1998).
[14] M. Cerny, M. Sob, J. Pokluda, and P. Sandera, J. Phys. Condens. Matter **16** 1045 (2004).
[15] H. Wang and M. Li, J. Phys. Condens. Matter **21**, 455401 (2009).
[16] H. Wang and M. Li, J. Phys. Condens. Matter **22**, 295405 (2010).
[17] J. R. Ray, Comput. Phys. Rep. **8**, 109 (1988).
[18] M. Li and W. L. Johnson, Phys. Rev. B **46**, 5237 (1992).
[19] F. Milstein and R. Hill, J. Mech. Phys. Solid. **27**, 255 (1979).
[20] F. Milstein and R. Hill, J. Mech. Phys. Solid. **26**, 213 (1978).
[21] F. Milstein and R. Hill, J. Mech. Phys. Solid. **25**, 457 (1977).
[22] R. Hill, Math. Proc. Camb. Phil. Soc. **77**, 225 (1975).
[23] R. Hill and F. Milstein, Phys. Rev. B **15**, 3087 (1977).
[24] J. W. Morris and C. R. Krenn, Phil. Mag. A **80**, 2827 (2000).
[25] H. Wang and M. Li, Phys. Rev. B **79**, 224102 (2009).
[26] Landolt-Börnstein, *Second and Higher Order Elastic Constants, New Series, Group III*, edited by A. G. Every and A. K. McCurdy (Springer-Verlag, Berlin, 1992), Vol. 29A.
[27] B. B. Karki, G. J. Ackland, and J. Crain, J. Phys. Condens. Matter **9**, 8579 (1997).
[28] D. Gerlich, J. Appl. Phys. **77**, 4373 (1995).
[29] Y. Hiki, J. R. Thomas, and A. V. Granato, Phys. Rev. **153**, 764 (1967).
[30] M. Cerny and J. Pokluda, J. Phys. Condens. Matter **21**, 145406 (2009).
[31] C. Krenn, D. Roundy, J. Morris, and M. Cohen, Mater. Sci. Eng. A **317**, 44 (2001).
[32] D. M. Clatterbuck, C. R. Krenn, M. L. Cohen, and J. W. Morris, Phys. Rev. Lett. **91**, 135501 (2003).